Communication

How Characterization of Particle Size Distribution Pre- and Post-Reaction Provides Mechanistic Insights into Mineral Carbonation [†]

Aashvi Dudhaiya and Rafael M. Santos * [iD]

School of Engineering, University of Guelph, Guelph, ON N1G 2W1, Canada; adudhaiy@uoguelph.ca

* Correspondence: santosr@uoguelph.ca; Tel.: +1-519-824-4120 (ext. 52902)

† Some contents of this paper also appear in the Proceedings of the 8th World Congress on Particle Technology Meeting (Orlando, USA, 2018), as extended abstract P508057, titled "Particle size characterization in mineral carbonation for understanding reaction fundamentals".

check for updates

Abstract: Mineral carbonation is the conversion of carbon dioxide, in gas form or dissolved in water, to solid carbonates. Materials characterization plays an important role in assessing the potential to use these carbonates in commercial applications, and also aids in understanding fundamental phenomena about the reactions. This paper highlights findings of mechanistic nature made on topics related to mineral carbonation, and that were made possible by assessing particle size, particle size distribution, and other morphological characteristics. It is also shown how particle size data can be used to estimate the weathering rate of carbonated minerals. An extension of the carbonation weathering rate approach is presented, whereby using particle size distribution data it becomes possible to predict the particle size below which full carbonation is obtained, and above which partial carbonation occurs. The paper also overviews the most common techniques to determine the particle size distribution, as well as complementary and alternate techniques. In mineral carbonation research, most techniques have been used as *ex situ* methods, yet tools that can analyze powders during reaction (*in situ* and real-time) can provide even more insight into mineral carbonation mechanisms, so researchers are encouraged to adopt such advanced techniques.

1. Introduction

Mineral carbonation is the conversion of carbon dioxide, in gas form or dissolved in water, to solid carbonates. These may include calcium carbonates, magnesium carbonates, and a variety of other alkaline earth metal carbonates. Alkaline earth metals can be derived from natural minerals, waste residues, or even brines [1]. When performed in a reactor, mineral carbonation leads to the formation of a powder that can be composed of a carbonate alone (e.g., high-purity precipitated calcium carbonate) [2], or a mixture of one or more carbonates with other solid phases, such as silica and silicates [3]. Materials characterization thus plays an important role in assessing the potential to use these carbonates in commercial applications (e.g., filler in paper, aggregate in concrete) [4]. Materials characterization also aids in understanding fundamental phenomena about the reactions, such as the behavior of the reagents, the formation of products and by-products, and the reaction rate and conversion limitations [5].

A materials characterization parameter regularly measured and reported is the particle size. This can include the particle size of the starting materials, or that of the converted minerals, at the end

of the reaction or as a function of the reaction extent. Particle size is expressed as an average value, as an interval, or as a distribution. Particle size data is used to predict the susceptibility of a mineral powder to carbonation, or to explain the mineral carbonation conversion achieved, or with eye towards materials applications. While experimental research on mineral carbonation can be conducted with little to no use of particle size characterization (though at a loss of mechanistic understanding of the reaction), knowledge of particle size is essential to the modeling of mineral carbonation reactions, an active area of research in recent years [6–9].

Gopinath and Mehra [6] modeled steel slag carbonation by assuming particles had a slab geometry, and used particle size information to describe not only the original and post-carbonation slab length, but also the location within the slab of the reaction front. They, notably, pointed out that when particle size distribution data is available, the conversion can be computed as a weighted average of the conversion in each bin, whereas when the distribution data is not available, the mean particle diameter is the next best data required. Pan et al. [7] reviewed several models to describe solid-liquid mineral carbonation reactions (shrinking core model, surface coverage model, integrated reaction-diffusion model, two-layer diffusion model, integrated transport-reaction model), all of which require information about particle size. The traditional shrinking core model can account for changes in particle size due to reaction products, using "Z factor" and "λ factor", but the modified shrinking core model reduces back to its original form when the particle size remains unchanged in the course of reaction [7,8]. The surface coverage model uses specific surface area of the reacting powder [9], which is related to the particle size for materials with low porosity and spheroidal shape (e.g., most slags), but can deviate significantly otherwise (e.g., fly ash), requiring dedicated determination.

This paper highlights (Section 3.1) the findings of the mechanistic nature that the corresponding author has made on topics related to mineral carbonation, and that were made possible by assessing particle size, particle size distribution, and other morphological characteristics. Similar applications of particle size characterization are also reviewed (Section 3.2) from recent works related to the carbonation of iron- and stainless-steel slags. Subsequently (Section 4.1), it is shown how particle size data can be used to estimate the weathering rate ($\mu m \cdot min^{-1}$) of carbonated minerals, which is a measure that normalizes carbonation conversion data with respect to volume-based average particle size, thus, making it possible to compare the carbonation of different materials using a particular process, or the carbonation of similar materials using different processes on an equal basis [10]. The carbonation weathering rate is also ideal for assessing the intensification efficacy of advanced carbonation methodologies [10,11]. An extension of the CWR approach is presented in Section 4.2, whereby using particle size distribution data it becomes possible to predict the particle size below which full carbonation is obtained, and above which partial carbonation occurs. The paper begins (Section 2) with an overview of the most common techniques to determine particle size distribution, as well as complementary and alternate techniques that provide additional particle size information and/or are able to record the particle size distribution *in situ* and under real process conditions.

2. Common, Complementary, and Alternate Particle Size Distribution Methodologies

2.1. Sieving Analysis

Sieving is classified as a mechanical method for particle size distribution (PSD) determination, and is the simplest and most often used method in minerals research. Sieving relies on the use of screens with specified mesh sizes to separate fractions of a (typically) dry powder sample. Particles pass through the sieve with the aid of vibrations, which can be manually generated, or using a vibratory shaker. The goal of these vibrations is to allow the smaller particles to travel downwards, by gravity, through the inter-particles spacing (porosity) around the larger particles. To achieve a high degree of separation (i.e., fractionation), the most important parameters during sieving are amplitude (e.g., 1.5 mm) and time (e.g., 5 min) of shaking, as well as having the correct amount of sample loaded onto the coarsest sieve [12].

Some important limitations of sieving reduce the value of this method for mineral carbonation research. One is that the smallest standard sieve size (400 mesh, or 0.036–0.038 mm) is significantly coarser than mineral particles often use for carbonation, especially when minerals are milled. The result is that researchers only know the passing fraction (e.g., 90 wt % passing 400 mesh), but not the exactle particle size distribution. Likewise, with coarser particles, it may be determined that a certain mass fraction of sample is between two mesh sizes in diameter (e.g., 25 wt % between 0.15 and 0.25 mm), but it is not possible to determine an exact value of average particle size even in this range, as the median value will only provide a rough estimate.

Another important issue with sieving, related to mineral carbonation research, is that fine particles can be trapped within coarser fractions, as a result of poor separation due to particle shape or electrostatic forces. This can skew the particle size distribution mass fractions determined but, most importantly, can affect experimental results. If a material contains fine particles, those particles will carbonate faster than the coarser particles, affecting the determination of reaction kinetics, especially with short carbonation durations. Wet sieving (with water or non-aqueous solvent) is a technique that can reduce fine particle entrapment, but can also lead to alteration of the particles (e.g., partial dissolution, hydration, caking) depending on the mineral.

Particle shape can also have an effect on sieving analysis results. The passage or the retention of a non-spherical particles, through or by a sieve of a given mesh size, is determined by the probability of the particle to assume an orientation relative to the mesh that allows it to pass through [13]; such an orientation exists when the particle's smallest cross-section is smaller than the sieve's aperture. The net outcome of the non-sphericity is that a coarser population is retained by a sieve than the actual population of particles with apparent diameters that match the sieve size [13].

Sieving, nonetheless, remains a valid laboratory technique as it can not only provide semi-quantitative particle size distribution information, but is also a solids separation technique. Mineral samples that are crushed, milled, sedimented, centrifuged, or precipitated can be passed through sieves to obtain a specific particle size fraction to be used for mineral carbonation reactions. These fractions can then be tested using advanced characterization techniques to accurately determine particle size distribution, average particle size, and particle shape.

2.2. Laser Diffraction Analysis

Laser diffraction analysis (LDA) is a technique that is useful to follow particle size growth or reduction. Thus, it can help elucidate effects of carbonation, such as the formation of precipitated layers or alteration of the microstructure, and of sonication (a technique to intensify the carbonation reaction), such as particle attrition and fragmentation. Of the three average particle diameters commonly obtained by laser diffraction (D50, D(4,3), and D(3,2)), the Sauter mean diameter (D(3,2)), being surface area sensitive, is the most important when it comes to the susceptibility towards mineral carbonation of powdery materials, since mineral carbonation reactivity is proportional to the exposed surface area. This mean diameter is also found to be the most sensitive to sonication effects, as it best detects the formation of micron- to sub-micron sized fragments. The volume-moment mean diameter (D(4,3)), on the other hand, is useful in indicating the degree of erosion of larger particles. These insights are discussed in more detail in Section 3.1.

The principle of laser diffraction analysis (LDA) is that particles of a given size diffract light through a given angle, which is inversely proportional to particle size, and the intensity of the diffracted beam at any angle is a measure of the number of particles with a specific cross-sectional area in the optical path [14]. For calculating particle sizes from the diffraction data, two techniques are commonly used: Fraunhofer diffraction and Mie theory. Both assume that the particles have a spherical shape (i.e., the particle dimension is the optical spherical diameter), but the Mie theory is deemed more accurate for clay-sized particles, hence, it is typically applied in mineral carbonation research [14]. Since laser diffraction inherently determines particle count, it is readily possible to present PSD data on a volume, surface area, or number basis, with the first being the most commonly reported and interpreted.

Determination of the particle size distribution (PSD) by LDA offers a number of advantages over sieving (and sedimentation, another long-established mechanical technique used in soil analysis). Most useful is its ability to generate a complete particle size distribution (i.e., a particle diameter histogram with small bin size), which, according to Fisher et al. [15], is important for: (1) more completely quantifying differences between samples; (2) developing mathematical functions to describe and utilize the PSD; and (3) transferring data between different particle size classification systems. LDA is also often cited as being a superior method for accurately determining particle diameter (i.e., closest to true value), and for more precisely differentiating between similar samples [16,17]. PSD data is also directly used to calculate average particle sizes, such as the volume median diameter (D50), the volume moment mean diameter (D(4,3)), and the surface area moment (Sauter) mean diameter (D(3,2)), or cumulative percentiles such as D10 or D90.

The operation of laser diffraction analyzer is best described by looking at the experimental procedure used in a specific study. Fisher et al. [15], in their study to compare LDA with the sedimentation-based sieve plummet balance technique, utilized a Malvern Mastersizer 2000 (Malvern Instruments, Malvern, UK) to carry out LDA, which uses a 52-detector array. Measurements were performed at a constant temperature of 20 °C (± 2 °C), and the samples were suspended and recirculated in water, with the pumping speed, stirring speed, and ultrasonic level set at 2000 rpm, 800 rpm, and 100%, respectively. Particle size was calculated on a volume basis using the Mie theory and Malvern proprietary software (version 5.6, Malvern Panalytical, Malvern, UK). The background measurements were taken for approximately 30 s, followed by measuring the suspended sample aliquot eight times (for replication) using a 30 s measurement duration each time, which is equivalent to 30,000 individual light scattering measurements. There are several factors that can affect the PSD obtained through LDA, including [15]: the number of detectors; the choice of measurement time; the samples preparation; and post-processing factors, such as the choice of Fraunhofer or Mie diffraction models, or the optical parameters used.

An important note made by Fisher et al. [15] is that LDA requires the suspension obscuration to be within a certain range (typically 10% to 20%), and this level of obscuration requires a small amount of sample (in the order of a gram, depending of particle size). For highly heterogeneous samples, it is, therefore, important to take and use representative samples to achieve this level of obscuration. Fisher et al. [15] achieved this with soils by using a precise wet riffling methodology. When available sample amounts are limited, on the other hand, LDA is far superior to mechanical methods, as even under low obscuration conditions (e.g., 2% to 10%), reasonable results can be obtained [15].

Another important limitation of LDA is that it does not accurately represent the size distribution of irregularly shaped particles [13], such as acicular crystals or fibrous minerals. The projected cross-sectional area of a non-spherical particle averaged over all possible orientations is larger than that of a sphere with an equal volume, which, for an entire population of non-spherical particles, leads to a shift of the PSD toward a coarser size [13]. Non-spherical particles can be either a feedstock (e.g., asbestos, wollastonite) or a product (e.g., aragonite, nesquehonite) in mineral carbonation reactions, so care must be taken when interpreting the PSD for these materials. This is especially important when making comparisons to PSDs obtained from other more spheroidal materials (e.g., precipitated aragonite versus calcite), or from PSDs of pre- or post-processing samples that have different morphology and size distribution.
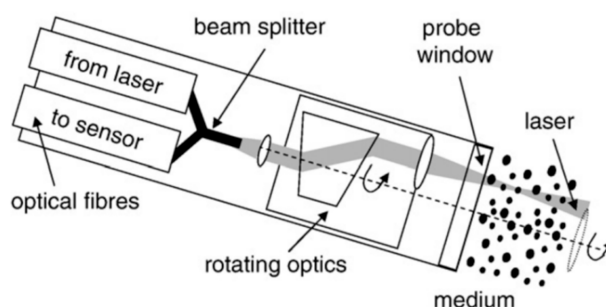
2.3. Complementary and Alternate Techniques (Laser Reflectance, Ultrasonic Extinction, Acoustic Spectrometry)

Sieving as a particle classification method and laser diffraction analysis as a particle size distribution and average particle size determination method are a useful pairing for most applications related to mineral carbonation research. However, other methodologies are available to provide either complementary information about particle size and shape or alternate testing techniques more suitable for particular applications. An important application is *in situ* particle size distribution

determination, such as in a pipe flow or stirred reactor. In situ methods allow testing of particles in their native environment, eliminating the need for sampling, filtration, drying, etc., all of which can alter particles or lead to unrepresentative sample. In situ methods also allow tracking of changes in particle size distribution (i.e., kinetics) while particles react, dissolve, precipitate, crystallize, agglomerate, de-agglomerate, fragment, etc. A key requirement of *in situ* PSD determination is that the particle suspension cannot be diluted for analysis, hence, making the application of laser diffraction more difficult than some alternate techniques briefly discussed hereafter. Optional requirements, especially for mineral carbonation research, may be operability under elevated pressures (e.g., 100–10,000 kPa) and temperatures (e.g., 0–200 °C).

2.3.1. Laser Reflectance

Focused beam reflectance measurement (FBRM) is a technique developed by Lasentec, now part of Mettler Toledo GmbH, which provides real-time measurement of the number and dimensions of particles *in situ* [18]. Its *in situ* capability is enabled by the measurement probe (Figure 1), which can be immersed in process fluids within conduits or vessels. Here, a laser beam rotates at a high speed and propagates into the particle suspension to be monitored. The presence of particles in the fluid is detected when a focused laser beam strikes a particle and backscatters into the probe. As the laser moves, a "cord length" is measured for the duration of the backscattering. The length of this scanned chord is recorded by the instrument for each particle it finds, and is transferred into a chord length distribution (CLD). In this way, CLD provides online particle count and particle dimension information. A CLD can be measured at every two seconds to track the dynamics of the process, multiple probes can be placed in the same reactor system, and the probe can withstand temperatures from −70 to 180 °C [18].

Figure 1. Schematic drawing of an FBRM probe [19]. Re-used with permission from Elsevier (4383110764877).

2.3.2. Ultrasonic Extinction/Acoustic Spectrometry

Another useful technique for real-time in-line (i.e., *in situ*) particle size distribution determination, in addition to solids loading (i.e., particle concentration) measurement, is known as ultrasonic extinction spectroscopy (UES), or acoustic spectrometry. As with FBRM, these techniques are also designed for applications where elevated pressures and temperatures are used within pipes or vessels, in addition to having high tolerance for aggressive chemical environments. UES is capable of detecting particles in the diameter range of 0.01 μm to 3000 μm, with solids concentrations up to 70 vol %, in opaque liquids and emulsions, and measures the frequency-dependent UE, which, as a result, enables calculation of both particle size distribution and particle concentration [20]. The principle of operation is as follows: particles smaller than the acoustic wavelength are detected by attenuation of ultrasonic intensity, while particles with diameter greater than the acoustic wavelength scatter the ultrasonic waves.

Extinction measurements are performed at multiple ultrasonic frequencies (i.e., wavelengths), and models are used to describe the viscous and thermal losses due to partial entrainment of the particles by the ultrasonic wave, thus generating an attenuation distribution as a function of particle

size, which provides both the PSD, as well as the solids concentration [20]. It is also possible to differentiate spherical and arbitrary shaped particles by empirically evaluating the extinction function. Geer and Witt [20] suggest that the particle size distribution be first measured by LDA, and the results be then mathematically combined with the measured ultrasonic extinction spectrum of the same sample. The aim of this kind of calibration procedure is to evaluate the extinction function only within the wave number limits given by the minimum and maximum particle size determined by LDA.

An important limitation of acoustic techniques is the relatively long spectrum acquisition, which is in the order of several minutes, which causes difficulties in real-time monitoring of PSD, such as when the flowing solids loading level fluctuates frequently [21]. DosRamos [21] also makes an important observation regarding real-time PSD monitoring for process control purposes, which is that PSD curves are not practical as set points. In turn, calculated mean particle diameter values (by volume, weight, surface area, or number) can be used as set-points, but can also be misleading since a single mean particle diameter (e.g., D(4,3) = 100 μm) can be produced by an infinite number of PSD curves, so product properties can change more quickly and more significantly than variations in D-values might suggest. This same caution is very applicable to mineral carbonation research, where authors can misinterpret their own results or the results of others when using mean D-values as a basis for discussion and even modeling. DosRamos [21] suggests that surface area average sizing data (i.e., D(3,2)) are less prone to sharp fluctuations from minor populations, and similarly percentile figures such as the D90 and, thus, can be more suitable as a set point for process control.

3. Discussion of PSD Utilization in Mineral Carbonation Research

3.1. Use of Particle Size Distribution In Carbonation Research of Santos et al.

In this section, mechanistic insights into mineral carbonation reactions, obtained through determination of PSD, are reviewed from three comprehensive studies published by Santos et al. [22–24] in recent years. The volume-based particle size distributions and the average particle diameters presented in this section have been determined by wet LDA (Malvern Mastersizer S) in sonicated deionized water, with a detection range of 0.06–878.7 μm.
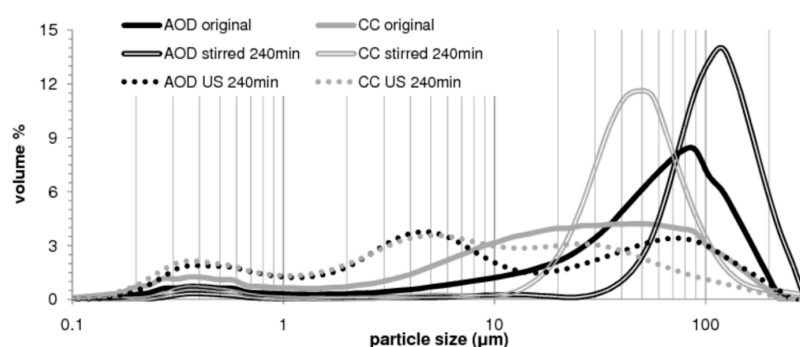
3.1.1. Ultrasound-Intensified Mineral Carbonation

Ultrasound has been investigated as a way to promote particle breakage during slurry carbonation, and to remove the carbonated shell or depleted matrix layers that surround the unreacted particle core, thus reducing diffusion limitations and exposing unreacted material to the aqueous phase [22]. Sonication (Hielscher UP200S, 24 kHz, 200 W, Hielscher Ultrasonics GmbH, Teltow, Germany) was shown to increase the conversion (94% vs. 86% over 25 min) and the process kinetics (0.65 vs. 0.59 g-$CaCO_3$/min) of calcium hydroxide carbonation, compared to mechanical stirring. Furthermore, particle size reduction of calcium hydroxide and carbonate powders is significantly greater than that of steel slag particles over 30 min of sonication (Table 1). This is likely a result of lower hardness, confirming the premise that sonication can clear the surface of unreacted mineral particles from the rate-limiting coverage of a carbonated shell.

Table 1. Particle size reduction by sonication, expressed as Sauter mean diameter [11]. Re-used with permission from John Wiley and Sons (4366260200646).

Powder	Original D(3,2) (μm)	Sonicated D(3,2) (μm)	Reduction (%)
$CaCO_3$ <200 μm	5.6	4.8	−14%
$CaCO_3$ 200–500 μm	25.7	6.4	−75%
$Ca(OH)_2$	1.8	0.9	−51%
CC slag <200 μm	2.6	2.5	−5%

LDA results have been particularly useful in assessing the performance of sonication as a means of process intensification. The effect of sonication on passivating layer removal from the surface of

carbonated slag particles was elucidated by the measurement of particle size distributions and electron microscopy imaging of particle morphology. Figure 2 shows volume-based particle size distributions of AOD (argon oxygen decarburization) and CC (continuous casting) slags before carbonation (original) and after four hours of carbonation with (US) and without (stirred) sonication. For both slags, similar shifts in particle size distributions take place. With stirring, the particle size distributions shift to larger particles; in fact, not only does it appear that large (10–100 μm) particles grow, it also appears that the amount of particles smaller than 10 μm decreases significantly, signifying that agglomeration/joining of carbonated particles takes place. In the case of sonication, the effect is the opposite: particle size distributions shift to smaller sizes, with clearly distinguishable creation of particles in the 0.2–1 μm and 2–10 μm ranges, and a reduction in the fraction greater than 10 μm. It can be theorized that the smallest particles (0.2–1 μm) are formed by flaking of the passivating layers, and the second mode (2–10 μm) is formed by the fragmentation of slag particles and/or are the eroded remains of once-larger slag particles.
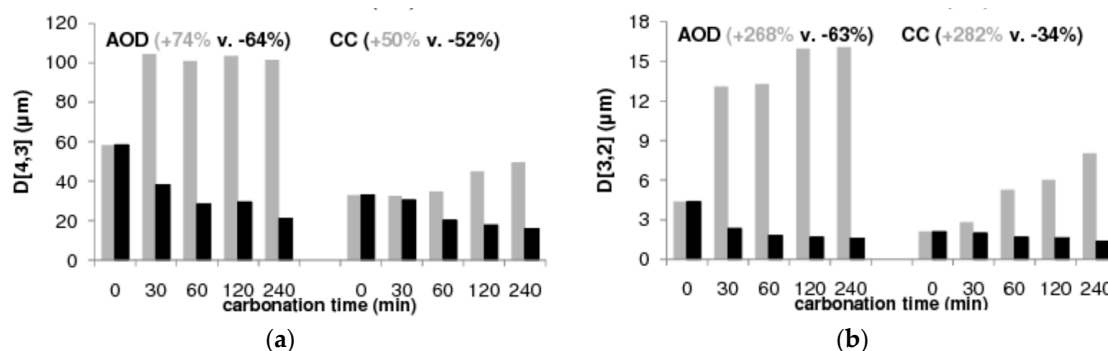

Figure 2. Particle size distributions of original and carbonated (240 min) powders of AOD and CC slags [22]. Re-used with permission from Elsevier (4366260475887).
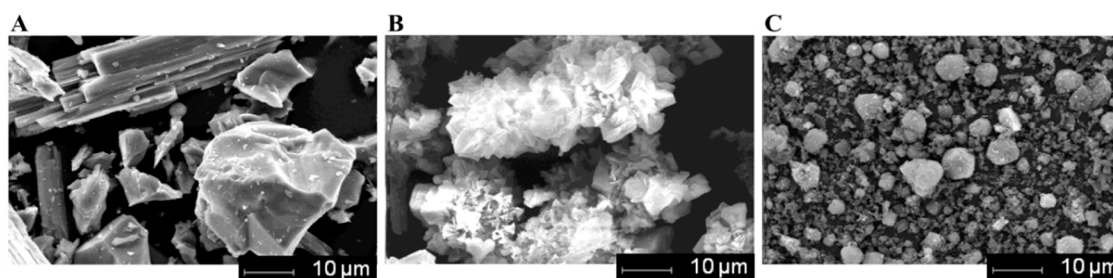
Figure 3 presents the average particles sizes of slag samples before and after carbonation as a function of reaction time. In the case of AOD slag under stirred carbonation, average particle sizes significantly increase after already 30 min of carbonation, but only D(3,2) increases further with the reaction time. This is in line with the fact that AOD carbonation with stirring reaches nearly maximum conversion in the first 30 min; subsequent increase in D(3,2) suggests aggregation of smaller particles with the larger ones. With sonication, however, average particle sizes progressively decrease as a function of time, indicating the continuing effect of ultrasound abrasion/milling. In the case of CC slag carbonation, average particle sizes progressively decrease with sonication, and increase without. It is interesting to note that CC particle size already clearly reduces after only 30 min of sonicated carbonation, when in the case of non-reacting sonication the particle size did not change (Table 1). This is suggestive that sonication removes not only the precipitated calcium carbonate layer, but also the depleted silica layer that once constituted the original slag particle material, and that this depleted silica layer is weaker than the original silicate material.

This has been further substantiated by comparing scanning electron microscopy (SEM, Philips XL30, Philips Electron Optics, Eindhoven, Netherlands) images to the LDA results. The morphology of CC slag particles prior and subsequent to carbonation is illustrated in Figure 4. As already indicated by particle size distributions, a clear distinction is seen between stirred and sonicated carbonation, and in relation to the original uncarbonated sample. In the case of stirred carbonation, the absence of particles smaller than 20 μm is confirmed, and the envelopment of slag particles in thick calcium carbonate layers, composed of rhombohedral calcite crystals, is validated. On the other hand, the sample subjected to sonicated carbonation exhibits distinguishably different morphology, being composed mainly of much smaller particles. Two modes are visible, in agreement with LDA results: flaky sub-micron particles, and rounded particles roughly 2–10 μm in size. It would appear that these

rounded particles are either remnants of larger particles that have been significantly eroded over time, or particles whose rugged corners have been polished by sonication. These results substantiate the supposition that ultrasound is capable of removal of passivating layers leading to exposure of unreacted particle core to the reacting solution, overcoming the rate/conversion limiting shrinking core phenomenon and contributing to the intensification of the mineral carbonation reaction. It is also worth noting that, while SEM provides direct visualization of particles, it is a semi-quantitative method for assessing the particle size distribution, while LDA is a quantitative method for doing so and, thus, offers added insight not realizable by SEM.

(a)   (b)

Figure 3. Average particle sizes (D(4,3) (**a**); D(3,2) (**b**)) of AOD and CC slags as a function of the carbonation time with stirred and sonicated carbonation; percentage values indicate the increase or decrease figures over four hours of carbonation [22]. Re-used with permission from Elsevier (4366260475887).

Figure 4. Comparison of particle morphology of original (**A**); stirred carbonated (**B**); and sonicated carbonated (**C**) CC slag powders [22]. Re-used with permission from Elsevier (4366260475887).

3.1.2. Synthesis of Pure Aragonite by Sonochemical Mineral Carbonation

LDA also provides a window into the mechanism that controls the particle size of sonochemically-synthesized aragonite precipitates (aragonite is the high-temperature polymorph of calcium carbonate). The formation of aragonite under sonication is attributable to two mechanisms: (i) imploding cavities generate localized regions of high temperature that can lead to the nucleation of aragonite seeds, given aragonite formation is promoted at higher temperatures; and (ii) the nucleation rate may be enhanced by sonication, thus maintaining stochastically preferable aragonite formation over calcite even at low crystal growth bulk temperatures.
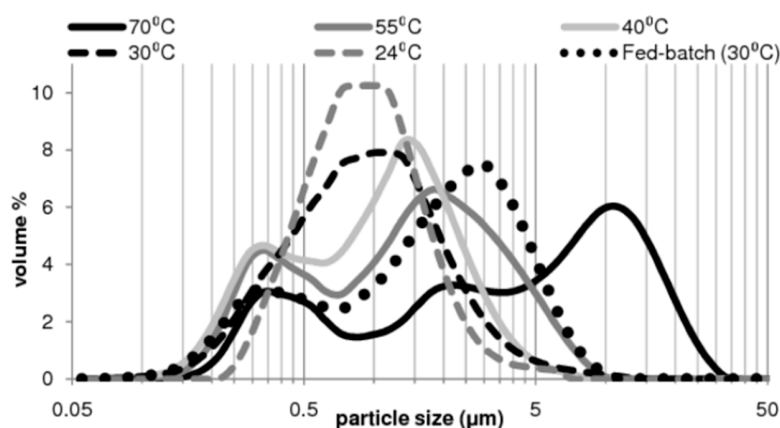
Pure aragonite precipitates were synthesized in this study [23] at a range of temperatures spanning from 24 °C to 70 °C. As was observed by SEM analysis, particle morphology changes as a function of temperature and so does particle size. Particle size and particle size distribution are important parameters of powder materials for certain industrial applications, such as paper coating or polymer filler; however, these data are not typically reported in literature for novel calcium carbonate morphologies, making it impractical to assess their suitability for industrial use. Table 2 lists average particle sizes by volume, expressed as D50 (mean volume diameter), D(3,2) (surface area moment

mean diameter) and D(4,3) (volume moment mean diameter), and Figure 5 shows the volume-based particle size distributions.

Table 2. Average particle sizes of pure aragonite synthesized with ultrasound at different temperatures [23]. Re-used with permission from Elsevier (4366260353846).

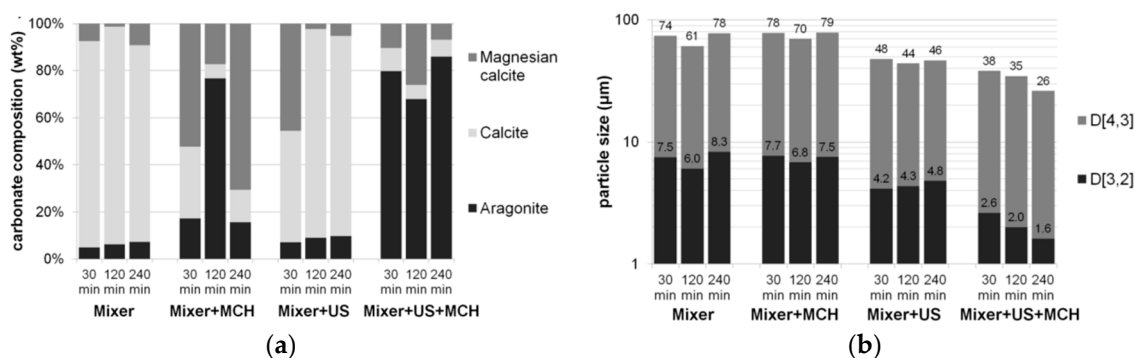| Temperature	D50	D(3,2)	D(4,3)	Aragonite
°C	µm	µm	µm	%
70 °C	4.15	1.31	6.48	99.5%
55 °C	1.33	0.78	1.87	98.7%
40 °C	0.98	0.65	1.27	98.6%
30 °C	0.85	0.69	1.23	99.3%
24 °C	0.84	0.79	1.09	98.6%
Fed-batch (30 °C)	1.74	0.87	2.22	96.7%

Figure 5. Particle size distributions of pure aragonite precipitates at varying temperatures [23]. Re-used with permission from Elsevier (4366260353846).

All samples presented in Figure 5 were synthesized with ultrasound and contain greater than 98% aragonite, as indicated in Table 2. In general, lowering the synthesis temperature results in shifting of the distribution to the left (smaller-sized); this is confirmed in Table 2 for the three listed size averages. The distributions of precipitates synthesized at higher temperatures have bimodal/trimodal characteristics, having a primary peak between 1 µm and 20 µm (and an intermediate peak at 2 µm for the 70 °C case) and a secondary peak below 1 µm. Larger particle modes are thought to represent needle-shaped particles, while the smaller modes may be fragmented particles, due to sonication, and/or particles that form near the end of the experiments when crystal growth becomes hindered by diminishing calcium concentration in solution. Samples from low temperature synthesis (24 °C and 30 °C) have unimodal distributions below 3 µm. The low temperatures, which may hinder crystal growth throughout the experiment, could be attributed to the smaller particle sizes. The fed-batch sample was found to have a bimodal distribution, likely comprised, as suggested by SEM imaging [23], of larger clustered crystals and smaller ultrasound-cleaved particles.

3.1.3. Self-Regenerative Additive for the Mineral Carbonation of Calcium-Rich Materials

When $MgCl_2$ is used as an additive during slag slurry carbonation, LDA helps to provide an explanation as to why $MgCl_2$ addition is only beneficial in the presence of sonication. Particle size reduction can be linked to the formation of acicular aragonitic crystals. In the case of sonicated experiments with $MgCl_2$, the preferential formation of aragonite, is clearly evidenced in Figure 6a; however, due to extensive attrition of the particles caused by sonication, the crystal morphology was not clearly discernible by SEM imaging [24]. Carbonate composition of Figure 6a was determined

by quantitative X-Ray diffraction ((QXRD, Philips PW1830, Philips Electron Optics, Eindhoven, The Netherlands), equipped with a graphite monochromator and a gas proportional detector, using Cu Kα radiation at 30 mA and 45 kV, mineral identification using Diffrac-Plus EVA (Bruker, version 3, Billerica, MA, USA) and mineral quantification performed by Rietveld refinement technique using Topas Academic (version 4.1, Coelho Software, Brisbane, Australia)).

Figure 6. Carbonate composition (**a**) and mean particle diameters (**b**) of carbonated AOD slag using mixer-only, combination mixer/ultrasound, with and without MCH addition, as a function of the reaction time; results with varying MCH dosages were averaged to facilitate plotting [24]. Re-used with permission from Elsevier (4366260286557).

The formation of aragonite can be tied to the further reduction in particle size for experiments combining ultrasound with MCH (Figure 6b). The use of ultrasound, without $MgCl_2$, reduces the volume moment mean diameter (D(4,3)) of the carbonated slag from the range of 61–78 μm to a range of 44–48 μm, and the surface area moment mean diameter (D(3,2)) from 6.0–8.3 μm to 4.2–4.8 μm. The addition of $MgCl_2$ to sonicated tests further reduces the D(4,3) and D(3,2) to as low as 26 and 1.6 μm, respectively, after 240 min reaction time.

These reductions are significant, and can be explained by two mechanisms: (i) the erosion of large particles is indicated primarily by the D(4,3) value (as it is sensitive to particle volume changes); and (ii) the formation of micron- to sub-micron sized fragments is reflected on the D(3,2) value (which is sensitive to the formation of surface area). It, thus, appears that aragonitic crystals, due to their acicular morphology and arrangement, are more easily cleaved off the surface of the carbonated particles due to sonication, compared to the more closely-packed calcitic layers formed in the absence of $MgCl_2$. This occurs either through the induction of cavitation shock waves and micro-jetting on the particle surface, or through enhanced inter-particle collisions.

3.2. Use of Particle Size Distribution by Various Other Slag Carbonation Researchers

In this section, mechanistic insights into mineral carbonation reactions involving iron- and steel-making slags, obtained through determination of particle size and/or PSD, are reviewed from several studies that have published in recent years from research groups around the world. Table 3 summarizes the methods used by these researchers to determine particle size and/or PSD, and how these data were used in the cited work, especially if significant mechanistic insight was obtained. The works reviewed in Table 3 are the same as the works that were reviewed by Georgakopoulos et al. [10] in a study that introduced and applied the carbonation weathering rate; for more on this topic, see Section 4.1. It is important to note that, to calculate the CWR, at least the volume-based average particle size must be known. If the PSD is also known, an extension of the CWR model, as discussed in Section 4.2, is possible.

Table 3. Summary of particle size determination methods and utilization from different carbonation studies reviewed by Georgakopoulos et al. [10].

	Type of Slag	Method of Particle Size Determination	How Particle Size/PSD Data Was Used
Huijgen et al. [25]	Basic Oxygen Furnace (BOF)	Sieving was used for particle size classification: ground slag was sieved into fractions: <38 μm, <106 μm, <200 μm, <500 μm, <2000 μm. Particle size distribution and volume-based mean particle size (D(4,3)) and $d_{0.5}$ of samples were measured, pre-carbonation, by laser diffraction (Malvern Mastersizer 2000) using ethanol (96%) as a dispersing agent.	It was noticed from PSD that all sample fractions had wide size distribution and all included very small particles <1 μm. It was suggested that since slag particles are non-porous, the specific surface area can be estimated using the D(4,3) value, rather than performing BET analysis. Carbonation conversion was inversely proportional to particle size, and it was found that the D(4,3) value can be fitted to the conversion data to yield a predictive exponential relationship.
Chang et al. [26]	BOF	Sieving was used for particle size classification: ground slag was sieved, with only materials passing a 44 μm mesh being used. SEM imaging was used, post-carbonation, to visualize particle size and shape.	SEM imaging qualitatively showed that particles shrank after carbonation, and that cubic particles of approximate 1–2 μm size, thought to be calcium carbonate, adhered to the surface of the remnants of slag particles. This was used as a sign that shrinking core model, with a protective carbonate layer around reacting particles, can describe the slag carbonation mechanism. The particle size (i.e., sieve mesh size) was used in a kinetic modeling equation fitted to the experimental data.
van Zomeren et al. [27]	BOF	Sieving was used for particle size classification: slags were air-cooled, broken and sieved to obtain the particle fraction in the range of 2–3.3 mm. Samples of carbonated slags were sieved, to <106 μm, before TGA analysis.	The size range of the pre-carbonation sieved slags corresponded to the size desired for aggregates, the intended application of carbonated slags. No discussion is made relating the particle size to experimental results.
Baciocchi et al. [28]	BOF	Sieving was used for particle size classification: slag was either directly sieved to <125 μm, or ball-milled followed by sieving to <150 μm.	No discussion is made relating to the particle size. Particle size, before and after grinding, appears in an equation to calculate the energy requirement to sequester one tonne of CO_2.
Chang et al. [29]	BOF	Sieving was used for particle size classification: dried slag was sieved to <88 μm. The particle size distribution of the slag, pre-carbonation, in tap water was obtained by laser diffraction (Malvern, Hydro 2000MU), which was adapted from the ISO 13320-1 method, with a range of 0.02–2000 μm. SEM imaging was used, post-carbonation, to visualize particle size and shape.	The value of the average particle size, determined from the PSD, was reported and compared to other studies. Particle size appears in an equation to model the reaction kinetics according to shrinking core model. SEM images showed small crystals of $CaCO_3$ on the surface of the reacting slag particles.

<div align="center">**Table 3.** *Cont.*</div>

	Type of Slag	Method of Particle Size Determination	How Particle Size/PSD Data Was Used
Chang et al. [30]	BOF	Sieving was used for particle size classification: dried slag was sieved to <44 μm. The particle size distribution of the slag, pre-carbonation, in tap water was obtained by laser diffraction (Malvern, Hydro 2000 MU), which was adapted from the ISO 13320-1 method, with a range of 0.02–2000 μm. SEM imaging was used, post-carbonation, to visualize particle size and shape.	The value of the average particle size, determined from the PSD, was only reported. SEM images showed small crystals of $CaCO_3$ on the surface of the reacting slag particles.
Polettini et al. [31]	BOF	The slag was separated through dry sieving into various size fractions, but only the 63−100 μm size class was investigated.	The choice of particle size fraction used was based on previous work, where the fraction chosen exhibited the highest carbonation yield.
Baciocchi et al. [32]	Stainless steel (SS)	Sieving was used for particle size classification: 0.425–2 mm (class A), 0.177–0.425 mm (class B), 0.105–0.177 mm (class C), < 0.105 mm (class D). Particle size distribution was determined, pre-carbonation, according to ASTM D422 standard procedure (withdrawn January 2016). The distribution of particle sizes larger than 75 μm (retained on the no. 200 sieve) was to be determined by sieving, while the distribution of particle sizes smaller than 75 μm was to be determined by a sedimentation process, using a hydrometer.	The particle size distribution curve indicated that the slag could be classified as sandy granular material. Loss on ignition (LOI) was performed on each size fraction, and it was found that finer fraction had greater LOI due to presence of hydroxide and carbonate species. Elemental composition was found to vary moderately depending on particle size, while pH only varied for the coarsest fraction, and mineralogy and leaching were similar for all fractions. Higher CO_2 uptake was achieved with smaller particle size, and this was attributed to increased surface area (not measured).
Tai et al. [33]	BOF	It is not mentioned how the reported particle size of the slag, 63–90 μm, was determined nor how this size fraction was obtained.	The particle size is only reported, with no further discussion or justification.
Baciocchi et al. [34]	Electric arc furnace (EAF)	The EAF slag was milled in a corundum ball mill to a particle size below 150 μm; the method of classification is not specified.	Particle size of two previous studies is also mentioned, but there is no discussion regarding particle size.

Table 3. *Cont.*

	Type of Slag	Method of Particle Size Determination	How Particle Size/PSD Data Was Used
Baciocchi et al. [35]	Argon Oxygen Decarburization (AOD)	The AOD slag, as received, as sieved to a particle size <150 μm, with 90% of the slag passing this mesh size. This study also used the same slag samples (SS and EAF) that were prepared by Baciocchi et al. [32] and by Baciocchi et al. [34].	Particle size was related to the elemental composition (heavy metals) of the different slags and fractions, and to their initial carbonate content, which was higher in the finer materials. Greater CO_2 uptake was found for finer SS slag fractions, and it was confirmed that milling of the coarsest SS fraction increases its CO_2 uptake. Maximum calcium conversions were estimated for each sieved size fraction, being highest for the finest fraction.
Chang et al. [36]	Blast Furnace (BF)	It is not mentioned how the reported particle size of the slag, 44 μm, was determined nor how this size fraction was obtained. SEM imaging was used, post-carbonation, to visualize particle size and shape.	Similar comments to those made in Chang et al. [29,30] regarding SEM images are made. A comparative table shows particle size of other studies, but no discussion about particle size is made.
Cappai et al. [37]	Waelz	The slag was crushed to a final particle size below 4 mm; the method of size classification is not mentioned.	Low carbonation conversion was associated to the coarse particle size used and, in turn, the low surface area of the slag, which is concluded to not favor the dissolution kinetics of reactive species. It is suggested that a pre-treatment stage based on particle size reduction could contribute to an optimized process.

A few conclusions and recommendations can be drawn from the summaries presented in Table 3. First, there is limited use of particle size and PSD characterization post-carbonation. As shown in Section 3.1, such post-carbonation analysis helps to undertand if carbonates are coating the surface of the slag, and also help to characterize the morphology and mineralogy of the products, especially if different polymorphs of calcium carbonate form, but also if precipitated or crystalized impurities from additives remain in the product powder. For the latter, particle size characterization should be combined with XRD or QXRD analysis, which are another class of analytical methods that can be more frequently used in slag carbonation research.

Another note that can be made from Table 3 is that most studies report particle size ranges, but neither the average size of each range nor the size distribution of each range is provided. As discussed by Georgakopolus et al. [10] the absence of precise particle size data makes the calculation of the CWR less accurate. It is also important to note that it is not possible to know with certainty if a slag sample classified as <44 μm is actually finer than one classified as <88 μm. Often times, these size classifications are given for ball milled slags. Ball milling is capable of reducing slag particles to a few micrometers or less, so the D(4,3) value of the <88 μm sample may easily be lower than that of the <44 μm samples, depending on the starting particle size prior to milling, the duration of milling, the size of balls, the filling ratio, etc. Another scenario is that of two samples reported as <150 μm, where one is ball milled then sieved, and the other directly sieved from an as-received or jaw-crushed slag. Here, the ball milled samples would likely have a much smaller D(4,3) value. None of the studies in Table 3 provide information about the sieving procedure such as how the pans were vibrated, for how long, and if any liquid was used to wash the sieved fractions, all of which affect the amount of entrained fines in the retained fractions. These types of uncertainties not only makes it difficult to calculate the CWR, but can cause misinterpretations of carbonation conversion or CO_2 uptake data, especially when comparing different studies.

The review of Table 3 is not all negative, however. Some unique recommendation and applications of particle size data, or insights obtained from it have been, at times, reported. Huijgen et al. [25] suggested that PSD data for non-porous materials can be used to obtain an adequate estimate of specific surface area, eliminating the need for cumbersome, and time-consuming, BET analysis. Baciocchi et al. [28] was the only studied that related particle size to energy requirement for CO_2 sequestration via slag carbonation, through an equation for milling energy requirement. In the field of mineral carbonation there is often a perception that milling is not feasible to develop a net CO_2-sequestering or economically sustainable process, but that perception is usually opinionative rather than mathematically quantified. On this topic, the only studied that correlated particle size to an intended application of the carbonated slag was that of van Zomeren et al. [27]. The use of slag as a carbon sink relies on regulations that force industry to develop treatment processes for their waste to reduce toxicity or environmental risk, or on carbon credits to off-set the cost of the carbonation process. Slag carbonation is more likely to be industrially implemented when the carbonated slags can be marketed as a useful product, such as aggregates for building materials. However, most commercial applications require materials with defined properties, and particle size (average and distribution) is often the first barrier to entry.

4. PSD Utilization in Mineral Carbonation Weathering and Conversion Models

4.1. Carbonation Weathering Rate Model

Although several studies on metallurgical slag carbonation have been conducted, a comparison of their reported reaction rate and conversion extent results has proven challenging. The main reason for this is that the slags used by the researchers have different particles sizes and, thus, different specific surface areas. Mineral carbonation is a solid-state-diffusion-limited process under most conditions, so the different particle sizes affect the carbonation rate and maximal achievable conversion. In order to make direct comparisons among the results obtained from different studies, the carbonation weathering

rate (CWR) was conceptualized [10]. The rate is expressed in units of $\mu m \cdot min^{-1}$, and represents the weathering rate of the particle radius, from the original outer radius of the slag particle to the final radius of the unreacted core of the carbonated slag particle. It is calculated according to Equation (1), where t_{carb} is the thickness of the carbonated shell of the particle, τ_{react} is the reaction time, r_x is the original average particle radius, and $C\%$ is the average particle conversion degree:

$$CWR = \frac{t_{carb}}{\tau_{react}} = \frac{r_x \cdot \left(1 - \sqrt[3]{1 - C\%/100\%}\right)}{\tau_{react}} \tag{1}$$

The CWR assumes that all reactive minerals carbonate at similar rates, that all particles are spherical, and does not account for the changing size of particles due to the accumulation of precipitated carbonates on the particle; that is, it only tracks the location of the reacted | unreacted interface. The second assumption is in principle not accurate, since the aspect ratio of iron- and steel-making slag particles is sometimes relatively high. However, laser diffraction is the typical technique used for determining average particle size, and this method does not distinguish particle shapes; therefore, the values used in the calculation of the CWR are already assumed to represent spherical particles. One limitation of the CWR is that it does not differentiate between weathering rate improvement due to particle size reduction and particle porosity enhancement. Thus, if a material is mechanically activated to improve carbonation, it will not be possible to distinguish between the two effects based on how the CWR responds.

By calculating the CWR from the carbonation conversions achieved by the studies that were reviewed by Georgakopoulos et al. [10], Table 4 was created. Some studies refer to the size of the slag particles as a range instead of a specific average mean diameter. In those cases, an arithmetic average of the range was taken as the mean diameter to calculate the CWR.

Table 4. Summary of slag and process parameters from different carbonation studies and the resulting calculated carbonation weathering rate (CWR) [10]. Re-used with permission from John Wiley and Sons (4366260073094).
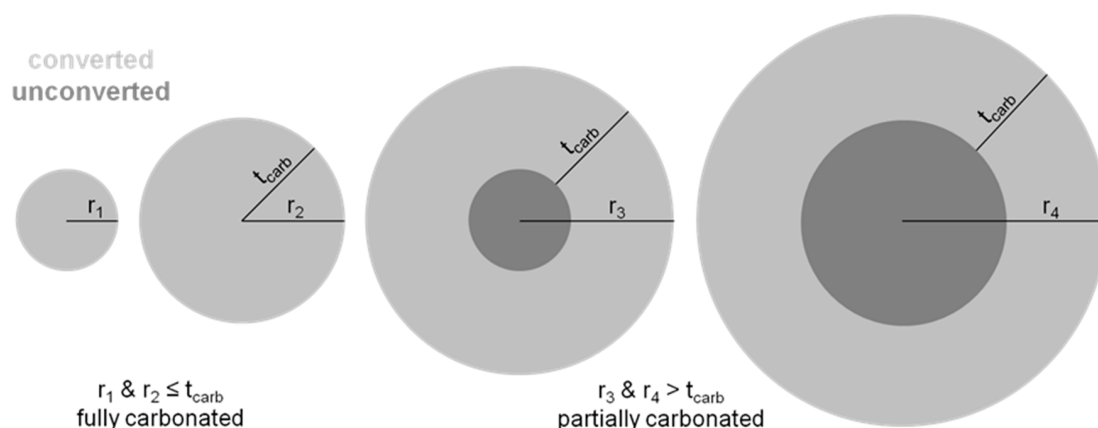
	Type of Slag	r_x (µm)	Conversion, $C\%$ (%)	t_{carb} (µm)	Reaction Time, τ_{react} (min)	CWR (µm/min)
Huijgen et al. [25]	BOF	19	74	6.87	30	0.229
Chang et al. [26]	BOF	22	68	6.95	60	0.116
van Zomeren et al. [27]	BOF	1000–1650	4.67	16.95–27.97	3600	0.004–0.007
Santos et al. [38]	BOF	40	36	5.53	30	0.184
Baciocchi et al. [28]	BOF(slurry)	75	40	11.74	1440	0.008
	BOF(wet)	62.5	20	4.48	1440	0.003
Chang et al. [29]	BOF	31	93.5	18.54	30	0.618
Chang et al. [30]	BOF	22	89.4	11.59	120	0.097
Polettini et al. [31]	BOF	31.5–50	53.6	7.11–11.29	240	0.030–0.047
Baciocchi et al. [32]	SS	52.5	27.2	5.26	480	0.011
Tai et al. [33]	BOF	31.5–45	65	9.30–13.29	60	0.155–0.221
Baciocchi et al. [34]	EAF(wet)	75	34.3	9.80	1440	0.007
	EAF(slurry)	75	25.4	7.00	240	0.029
Baciocchi et al. [35]	AOD	75	69.9	50.73	1440	0.017
Santos et al. [22]	AOD(mechanical)	30–115	30.5	3.43–13.14	240	0.0143–0.0547
	CC(mechanical)	30–115	61.6	8.20–31.41	240	0.0341–0.1309
	AOD(sonication)	30–115	48.5	5.95–22.82	240	0.025–0.095
	CC(sonication)	30–115	73.2	10.66–40.86	240	0.044–0.170
Santos et al. [5]	AOD(wet)	23.05	24.2	2.03	8640	0.000235
	CC(wet)	19.65	37	2.81	8640	0.000325
	AOD(slurry)	23.05	44	4.05	60	0.068
	CC(slurry)	19.65	57	4.82	60	0.080
Chang et al. [36]	BF	22	68.3	7.00	720	0.010
Cappai et al. [37]	Waelz	2000	18.3	130.46	14400	0.009

As an overall observation, it is clearly shown that the highest carbonation conversions do not necessarily correspond to the highest CWR. It is worthwhile to point out the electric arc furnace (EAF) slag study conducted by Baciocchi et al. [34]. It is one of the few cases in the literature where wet (thin-film) carbonation of a particular slag results in a higher conversion extent than when using

the slurry route. However, the CWR calculated for the wet route is remarkably lower than that for the slurry route (0.010 μm/min for wet carbonation, versus 0.046 μm/min for slurry carbonation), indicating that the slurry route is the more time-efficient way for carbonation. In fact, the higher conversion that was achieved by the wet route could be attributed to the longer period of carbonation (6 days vs. 6 h). This comparison confirms the usefulness of the CWR calculation in delivering more accurate and insightful results, as opposed to simple CO_2 uptake or conversion extent, since the CWR takes the reaction period into consideration, in addition to the particle size.

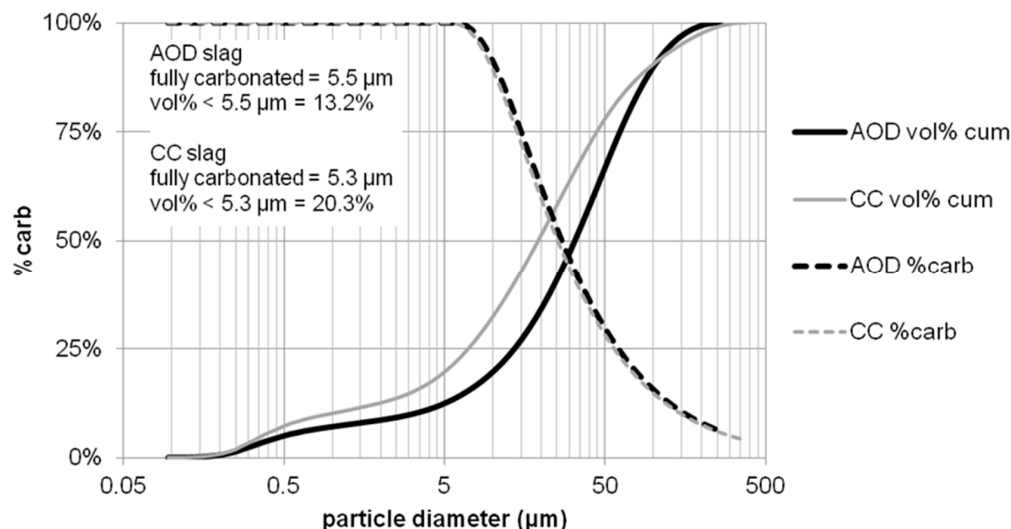### 4.2. Modeling Mineral Carbonation Conversion Based on PSD and CWR

Another use of the CWR calculation, introduced in the doctoral thesis of Santos [39], is to know what maximum mineral particle size achieves full carbonation, and starting from which particle size is only partial carbonation achievable. Figure 7 illustrates these two theoretical cases. The first two particles from the left reach full carbonation since the particle radius (r_x) is less than, or equal, to the converted thickness (t_{carb}). The last two particles on the right are only partially carbonated since the particle radius is greater than the converted thickness. In this case, it is possible to estimate the particle conversion degree (*%carb*), which simply equals the ratio between the volume of the carbonated hollow sphere, over the volume of the entire particle sphere. It should be noted that this model has two important assumptions: first, it assumes all mineral phases carbonate equally and, second, it does not take into account the increasing particle size due to the accumulation of carbonate crystals on the surface of the particle (i.e., t_{carb} is expected to be larger than the calculated value, although this simplification does not significantly affect the estimated radius of the unconverted particle core ($r_x - t_{carb}$)).

Figure 7. Theoretical model of physical carbonation conversion extent for particles of different size (see text for the description of the assumptions made) [39].

Using Equation (2), together with (i) the PSDs of AOD and CC slag obtained by laser diffraction [39]; and (ii) the maximal overall carbonation degrees of AOD and CC slags of 50% and 60%, respectively, obtained by thermogravimetric analysis [39], it is possible to estimate the particle size below which full carbonation may occur, and above which only partial carbonation occurs. Furthermore, it is possible to estimate the carbonation conversion degree as a continuous function of particle size. The modelling results, together with particle size distributions, are presented in Figure 8, and the calculation spreadsheet, including particle size data, is provided in the Supplementary Material.

$$\%carb = \begin{cases} if[r_x \leq t_{carb}], = 100\% \\ if[r_x > t_{carb}], = \dfrac{\frac{4}{3}\pi r_x^3 - \frac{4}{3}\pi(r_x - t_{carb})^3}{\frac{4}{3}\pi r_x^3} \end{cases} \tag{2}$$
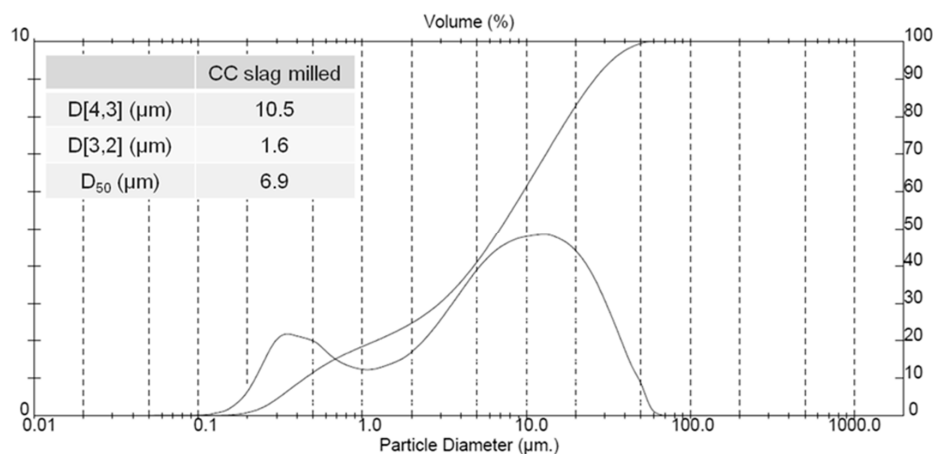
Figure 8. Particle size distribution of fresh AOD and CC slags (vol % cum), determined by laser diffraction, and modelling results of particle carbonation conversion degrees (%carb) [39].
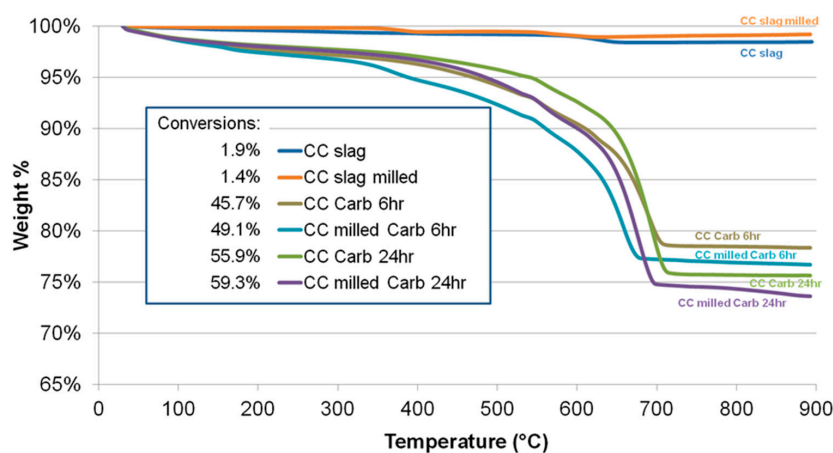
It is found that the estimated particle size for full carbonation conversion is very similar for the two slags, 5.5 and 5.3 μm for AOD and CC slags, respectively. Taking into account that CC slag possessed 20.3 vol % of particles below 5.3 μm, while AOD slag possessed only 13.2 vol % of particles below 5.5 μm, this helps explain why the overall carbonation degree of CC slag is greater than AOD slag. Beyond these particle diameter values, the conversion degree of both slags drops as the particle diameter increases, crossing the 50% mark at around 26 μm, and the 25% mark at around 60 μm. Interestingly, despite slightly different particle size distributions, the *%carb* curves overlap each other almost precisely. This is an indication that this model has good validity, despite the assumptions previously discussed. What this model shows is that, if a certain carbonation extent is desired for all particles, in view of slag stabilization or valorization, it may be possible to physically separate the greater proportion of well-carbonated (and, thus, likely stabilized) particles from the poorly-carbonated particles (or alternatively sieve the slag prior to carbonation). This approach would result in a valorizable fine product batch, and a smaller batch containing coarse unstabilized slag that may be disposed of at reduced cost, or be more easily valorizable due to the removal of fines.

In order to confirm if particle size is a more important factor in limiting carbonation degree versus mineralogy, a carbonation test was performed on finely-milled CC slag, prepared using a McCrone Micronizing Mill. The particle size distribution of this material is presented in Figure 9. The D50 value of this material is about one third that of the original slag (20.2 μm), the surface-specific D(3,2) value is 42% smaller, and >99.9 vol % of the material is below 60 μm (the value previously estimated for 25% conversion).

Pressurized slurry carbonation tests were conducted with original and milled CC slags for the determination of the particle size reduction effect on carbonation conversion. The processing conditions used were mild (60 °C, 300 kPa, CO_2, 20 g solids in 800 mLDI water, 1000 rpm stirring), while reaction durations were comparatively long (6 and 24 h). Thermogravimetric analysis curves and calculated conversions are presented in Figure 10. Milling improved carbonation conversion by 3.4%, both after 6 and 24 h. Still, conversion evidently did not reach full extent. Even considering only the calcium content of CC slag to calculate conversion (seeing that carbonation conditions might have been too mild to fully react the magnesium content), the conversion obtained after 24 h using the milled material is still limited to 75%. This emphasizes that mineralogical and microstructual effects also play an important role in limiting conversion, which is an important conclusion in view of possible future efforts to engineer slags and other thermal residues for high reactivity as carbon sinks.

Figure 9. Particle size distribution of micronized CC slag, determined by laser diffraction [39].

Figure 10. Pressurized slurry carbonation results of original and milled CC slag, determined by thermogravimetric analysis; CO_2 uptake calculated as weight loss between 300 and 750 °C [39].

5. Conclusions

The purpose of this paper was to highlight how particle size distribution characterization can be used in mineral carbonation studies to provide complimentary data and insight when used in combination with other techniques, such as scanning electron microscopy (SEM) and quantitative X-ray diffraction (QXRD). While particle size analysis, such as LDA, is a morphological assessment tool, it can aid in understanding a variety of chemical and mineralogical phenomena and mechanisms. The LDA technique has been used in most of the reviewed examples as an *ex situ* method, that is, to analyze materials before or after reaction. There are now particle size analysis tools that can analyze powders during reaction (*in situ* and real-time), under elevated temperatures and pressures. These techniques utilise laser diffraction (Malvern Instruments, Malvern, United Kingdom), dynamic imaging (Sopat, Berlin, Germany; PS Prozesstechnik GmbH, Basel, Switzerland), ultrasonic extinction (Sympatec GmbH, Clausthal-Zellerfeld, Germany), acoustic spectrometry (Dispersion Technology, Bedford Hills, NY, USA), and laser reflectance (Mettler Toledo, Columbus, OH, USA) methodologies. Even more insight into mineral carbonation mechanisms than *ex situ* LDA can provide is, thus, possible, so researchers are encouraged to adopt such advanced techniques. At the very least, mineral carbonation research stands to benefit from the incorporation of LDA analysis, and the determination and utilisation of full-range, continuous PSD, pre- and post-reaction, into most works.

Supplementary Materials: The following are available online at http://www.mdpi.com/2076-3263/8/7/260/s1, Spreadsheet containing the raw data and calculation to generate Figure 8 data.

References

1. Bodor, M.; Santos, R.M.; Van Gerven, T.; Vlad, M. Recent developments and perspectives on the treatment of industrial wastes by mineral carbonation—A review. *Cent. Eur. J. Eng.* **2013**, *3*, 566–584. [CrossRef]
2. De Crom, K.; Chiang, Y.W.; Van Gerven, T.; Santos, R.M. Purification of slag-derived leachate and selective carbonation for high-quality precipitated calcium carbonate synthesis. *Chem. Eng. Res. Des.* **2015**, *104*, 180–190. [CrossRef]
3. Santos, R.M.; Knops, P.C.M.; Rijnsburger, K.L.; Chiang, Y.W. CO_2 Energy Reactor—Integrated Mineral Carbonation: Perspectives on Lab-Scale Investigation and Products Valorization. *Front. Energy Res.* **2016**, *4*, 5. [CrossRef]
4. Bodor, M.; Santos, R.M.; Cristea, G.; Salman, M.; Cizer, Ö.; Iacobescu, R.I.; Chiang, Y.W.; Van Balen, K.; Vlad, M.; Van Gerven, T. Laboratory investigation of carbonated BOF slag used as partial replacement of natural aggregate in cement mortars. *Cem. Concr. Compos.* **2016**, *65*, 55–66. [CrossRef]
5. Santos, R.M.; Van Bouwel, J.; Vandevelde, E.; Mertens, G.; Elsen, J.; Van Gerven, T. Accelerated mineral carbonation of stainless steel slags for CO_2 storage and waste valorization: Effect of process parameters on geochemical properties. *Int. J. Greenhouse Gas Control* **2013**, *17*, 32–45. [CrossRef]
6. Gopinath, S.; Mehra, A. Carbon sequestration during steel production: Modelling the dynamics of aqueous carbonation of steel slag. *Chem. Eng. Res. Des.* **2016**, *115*, 173–181. [CrossRef]
7. Pan, S.-Y.; Ling, T.-C.; Park, A.-H.A.; Chiang, P.-C. An Overview: Reaction Mechanisms and Modelling of CO_2 Utilization via Mineralization. *Aerosol Air Qual. Res.* **2018**, *18*, 829–848. [CrossRef]
8. Pan, S.-Y.; Liu, H.-L.; Chang, E.-E.; Kim, H.; Chen, Y.-H.; Chiang, P.-C. Multiple model approach to evaluation of accelerated carbonation for steelmaking slag in a slurry reactor. *Chemosphere* **2016**, *154*, 63–71. [CrossRef] [PubMed]
9. Ji, L.; Yu, H.; Yu, B.; Zhang, R.; French, D.; Grigore, M.; Wang, X.; Chen, Z.; Zhao, S. Insights into Carbonation Kinetics of Fly Ash from Victorian Lignite for CO_2 Sequestration. *Energy Fuels* **2018**, *32*, 4569–4578. [CrossRef]
10. Georgakopoulos, E.; Santos, R.M.; Chiang, Y.W.; Manovic, V. Influence of process parameters on carbonation rate and conversion of steelmaking slags – Introduction of the 'carbonation weathering rate'. *Greenh. Gases Sci. Technol.* **2016**, *6*, 470–491. [CrossRef]
11. Santos, R.M.; Van Gerven, T. Process intensification routes for mineral carbonation. *Greenh. Gases Sci. Technol.* **2011**, *1*, 287–293. [CrossRef]
12. Żegleń, K.; Grygier, D.; Ambroziak, A.; Tulej, M. Particle size distribution determination methods comparison based on sieve analysis and laser method. *Interdiscip. J. Eng. Sci.* **2016**, *4*, 19–23.
13. Eshel, G.; Levy, G.J.; Mingelgrin, U.; Singer, M.J. Critical evaluation of the use of laser diffraction for particle-size distribution analysis. *Soil Sci. Soc. Am. J.* **2004**, *68*, 736–743. [CrossRef]
14. Di Stefano, C.; Ferro, V.; Mirabile, S. Comparison between grain-size analyses using laser diffraction and sedimentation methods. *Biosyst. Eng.* **2010**, *106*, 205–215. [CrossRef]
15. Fisher, P.; Aumann, C.; Chia, K.; O'Halloran, N.; Chandra, S. Adequacy of laser diffraction for soil particle size analysis. *PLoS ONE* **2017**, *12*, e0176510. [CrossRef] [PubMed]
16. Goossens, D. Techniques to measure grain-size distributions of loamy sediments: A comparative study of ten instruments for wet analysis. *Sedimentology* **2008**, *55*, 65–96. [CrossRef]
17. Roberson, S.; Weltje, G.J. Inter-instrument comparison of particle-size analysers. *Sedimentology* **2014**, *61*, 1157–1174. [CrossRef]
18. Worlitschek, J.; de Burh, J. *Crystallization Studies with Focused Beam Reflectance Measurement and Multimax. Application Note, AutoChem, MultiMax*; Mettler Toledo: Schwerzenbach, Switzerland, 2005; pp. 1–13.
19. Kail, N.; Briesen, H.; Marquardt, W. Analysis of FBRM measurements by means of a 3D optical model. *Powder Technol.* **2008**, *185*, 211–222. [CrossRef]

20. Geers, H.; Witt, W. *Ultrasonic Extinction for in-line Measurement of Particle size and Concentration of Suspensions and Emulsions*; Particulate Systems Analysis 2003: Harrogate, UK, 2003; pp. 1–5.

21. DosRamos, J.G. Acoustic attenuation spectroscopy for process control of dispersed systems. *IOP Conf. Ser. Mater. Sci. Eng.* **2012**, *42*, 012023. [CrossRef]

22. Santos, R.M.; François, D.; Mertens, G.; Elsen, J.; Van Gerven, T. Ultrasound-intensified mineral carbonation. *Appl. Therm. Eng.* **2013**, *57*, 154–163. [CrossRef]

23. Santos, R.M.; Ceulemans, P.; Van Gerven, T. Synthesis of pure aragonite by sonochemical mineral carbonation. *Chem. Eng. Res. Des.* **2012**, *90*, 715–725. [CrossRef]

24. Santos, R.M.; Bodor, M.; Dragomir, P.N.; Vraciu, A.G.; Vlad, M.; Van Gerven, T. Magnesium chloride as a leaching and aragonite-promoting self-regenerative additive for the mineral carbonation of calcium-rich materials. *Miner. Eng.* **2014**, *59*, 71–81. [CrossRef]

25. Huijgen, W.J.J.; Comans, R.N.J.; Witkamp, G.J. Mineral CO_2 sequestration by steel slag carbonation. *Environ. Sci. Technol.* **2005**, *39*, 9676–9682. [CrossRef] [PubMed]

26. Chang, E.E.; Chen, C.H.; Chen, Y.H.; Pan, S.Y.; Chiang, P.C. Performance evaluation for carbonation of steel-making slags in a slurry reactor. *J. Hazard. Mater.* **2011**, *186*, 558–564. [CrossRef] [PubMed]

27. van Zomeren, A.; van der Laan, S.R.; Kobesen, H.B.A.; Huijgen, W.J.J.; Comans, R.N.J. Changes in mineralogical and leaching properties of converter steel slag resulting from accelerated carbonation at low CO_2 pressure. *Waste Manag.* **2011**, *31*, 2236–2244. [CrossRef] [PubMed]

28. Baciocchi, R.; Costa, G.; Polettini, A.; Pomi, R.; Stramazzo, A.; Zingaretti, D. Accelerated Carbonation of Steel Slags Using CO_2 Diluted Sources: CO_2 Uptakes and Energy Requirements. *Front. Energy Res.* **2016**, *3*, 56. [CrossRef]

29. Chang, E.E.; Pan, S.Y.; Chen, Y.H.; Tan, C.S.; Chiang, P.C. Accelerated carbonation of steelmaking slags in a high-gravity rotating packed bed. *J. Hazard. Mater.* **2012**, *227*, 97–106. [CrossRef] [PubMed]

30. Chang, E.E.; Chiu, A.C.; Pan, S.Y.; Chen, Y.H.; Tan, C.S.; Chiang, P.C. Carbonation of basic oxygen furnace slag with metalworking wastewater in a slurry reactor. *Int. J. Greenh. Gas Control* **2013**, *12*, 382–389. [CrossRef]

31. Polettini, A.; Pomi, R.; Stramazzo, A. Carbon sequestration via steel slag accelerated carbonation: The influence of operating conditions on process evolution and yield. In Proceedings of the 5th International Conference on Accelerated Carbonation for Environmental and Material Engineering (ACEME), New York, NY, USA, 21–24 January 2015; pp. 1–30.

32. Baciocchi, R.; Costa, G.; Polettini, A.; Pomi, R. Influence of particle size on the carbonation of stainless steel slag for CO_2 storage. *Energy Procedia* **2009**, *1*, 4859–4866. [CrossRef]

33. Tai, C.I.; Su, C.Y.; Chen, Y.T.; Shih, S.M.; Chien, W.C. Carbonation of natural rock and steel slag using supercritical carbon dioxide. In Proceedings of the 11th European Meeting on Supercritical Fluids, Barcelona, Spain, 4–7 May 2008; pp. 1–6.

34. Baciocchi, R.; Costa, G.; Di Bartolomeo, E.; Polettini, A.; Pomi, R. Wet versus slurry carbonation of EAF steel slag. *Greenh. Gases Sci. Technol.* **2011**, *1*, 312–319. [CrossRef]

35. Baciocchi, R.; Costa, G.; Di Bartolomeo, E.; Polettini, A.; Pomi, R. Carbonation of Stainless Steel Slag as a Process for CO_2 Storage and Slag Valorization. *Waste Biomass Valorization* **2010**, *1*, 467–477. [CrossRef]

36. Chang, E.E.; Pan, S.Y.; Chen, Y.H.; Chu, H.W.; Wang, C.F.; Chiang, P.C. CO_2 sequestration by carbonation of steelmaking slags in an autoclave reactor. *J. Hazard. Mater.* **2011**, *195*, 107–114. [CrossRef] [PubMed]

37. Cappai, G.; De Giudici, G.; Medas, D.; Muntoni, A.; Nieddu, A.; Orrù, G.; Piredda, M. Carbon dioxide sequestration by accelerated carbonation of Waelz slag. In Proceedings of the 5th International Conference on Accelerated Carbonation for Environmental and Material Engineering (ACEME), New York, NY, USA, 21–24 June 2015; pp. 1–34.

38. Santos, R.M.; Ling, D.; Sarvaramini, A.; Guo, M.; Elsen, J.; Larachi, F.; Beaudoin, G.; Blanpain, B.; Van Gerven, T. Stabilization of basic oxygen furnace slag by hot-stage carbonation treatment. *Chem. Eng. J.* **2012**, *203*, 239–250. [CrossRef]

39. Santos, R.M. Sustainable Materialization of Residues from Thermal Processes into Carbon Sinks. Ph.D. Thesis, Katholieke Universiteit Leuven, Leuven, Belgium, 2013.